Proceedings of the 2011 IEEE
International Conference on Mechatronics
April 13-15, 2011, Istanbul, Turkey

Modeling and Control of a One-Legged Hopping Mechanism

Mesut Acar[#1], Zeki Yağız Bayraktaroğlu[#2]

[#]*Mechanical Engineering Department, Istanbul Technical University*
Gümüşsuyu, İstanbul, Turkey
[1]acarmes@itu.edu.tr
[2]zeki.bayraktaroglu@itu.edu.tr

Abstract— **This paper deals with one-legged jumping motion with a model of 3-DoF leg with foot. Equations of motion are derived through the Lagrange method and a soft contact model is used in computation of the contact forces between the foot and ground. Flight and stance phases of jumping motion are separately investigated and specific controllers are proposed for each phase. Flight phase control is considered as a servo positioning problem while stance phase control is considered as a force control problem. In controller design, total mass of the articulated leg is assumed to be concentrated at the hip level and a fictitious spring is assumed to operate between the hip and ankle joints. The approach is evaluated by taking into account dynamic balance with Zero Moment Point.**

***Keywords*— Legged locomotion, one-legged hopping**

I. INTRODUCTION

Legged locomotion has become one of the most attractive fields in robotics research in the last few decades. Intensive developments have been achieved in both theory and practice with several sophisticated walking and running robots. ASIMO developed by Honda [1], HRP by METI [2], Johnnie by TUM [3], and BigDog by Boston Dynamics Inc. [4] are some examples to those biped and humanoid robots. A major challenge in biped locomotion is dynamically balanced walking and all of these prototypes have achieved dynamically balanced walking and some of them have also achieved running motion.

Running motion differs from the walking by a flight phase which introduces new challenges in design and control of dynamically balanced running robots. First of all, landing and take-off instants of the feet have a dominant effect on the dynamics of the running robot because of rapid changes in contact forces. Secondly, during the flight phase the robot is a free flying mechanism therefore control techniques relying on "fixed base manipulator" assumption cannot be applied. Thirdly, power requirement of running is greater than that of walking, which constitutes a major constraint in design of mechanisms.

Theoretical and practical aspects of running motion have been investigated by several researchers. Raibert has developed one, two and four-legged running robots [5]. These robots consist of telescopic legs with point contact with the ground. A simple three-term control algorithm has been used in motion control. Running and somersault movements have been achieved by these robots. Kajita studied running pattern generation for a versatile humanoid robot [6]. His studies are focused on humanoids with rigid links and joints. Kawamura applied a virtual spring principle for generating jumping patterns for a biped robot [7]. Uğurlu generated running patterns based on ZMP and Euler equations [8]. Nagasaka developed a small jumping and running humanoid [9].

The swing phase in walking is replaced by a flight phase in running. Both phases start with take-off and end with landing of the foot. Walking and running exhibits both similar periodic motions and the same symmetry characteristics in motions of right and left legs. Therefore the dynamic behavior of one-legged jumping seems to be fundamental in the analysis of bipedal jumping and running. Many one-legged models and prototypes have been proposed [10]. Tajima developed an articulated one-legged robot [11, 12].

In this paper, a planar one-legged hopping mechanism model and related controllers are proposed. Modeling of the mobile mechanism and ground contact are represented in Section II. Flight and stance phase controllers as well as force control approach and virtual spring principle used in derivations are described in Section III. Section IV represents the simulation results and a brief description is given in the last section.

II. MODELING

A. System Description

The robot model is a 4-link, 3-joint, 6-DoF mechanism free to move in the x-z plane. The generalized coordinates are $x,\ z,\ \beta,\ \theta_1, \theta_2$, and θ_3. x and z represent the ankle position in the plane, β the orientation of the foot in the plane, and θ_1, θ_2, and θ_3 the joint angles. Active forces acting on the system are joint torque τ_1, τ_2, τ_3, normal contact forces are f_{cz1}, f_{cz2} and friction forces at contacts are f_{cx1}, f_{cx2}. Links are numbered 0 to 3 and joints are numbered 1 to 3 from foot to body. Two reference frames are attached to each link. Arrangement of the reference frames $\{O_i\}$ relative to links is shown in Fig. 1. Frames $\{O_{C_i}\}$ are attached at the center of mass of links. $\{O_b\}$ is a fixed reference frame. H_1 and H_2 are the contact points of the foot with the ground.

B. Contact Model

As mentioned in the previous section, the robot is modelled as a free flying mechanism. However during stance phases, the foot of the mechanism has a unilateral contact with the

978-1-61284-985-0/11/$26.00 ©2011 IEEE

ground through the points H_1 and H_2. Therefore a contact model must be utilized to compute the contact forces between the foot and ground. In this work, a so-called soft contact model is used in calculation of the contact forces [13]. The ground surface is compliant in both normal and tangential directions while the foot is considered as a rigid body. The generalized coordinates for the ground surface are x_g and z_g. The spring/damper constants along normal and tangential directions are represented respectively by K_n/D_n and K_t/D_t. The proposed contact model is shown in Fig. 2.

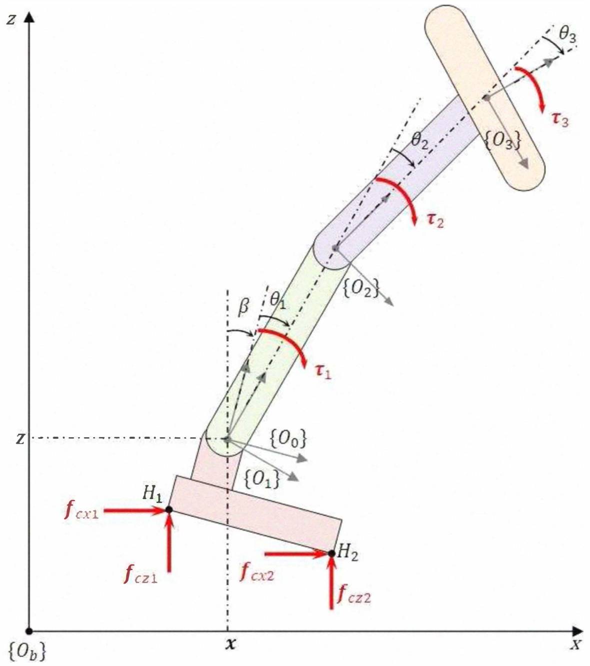

Fig. 1 System Description

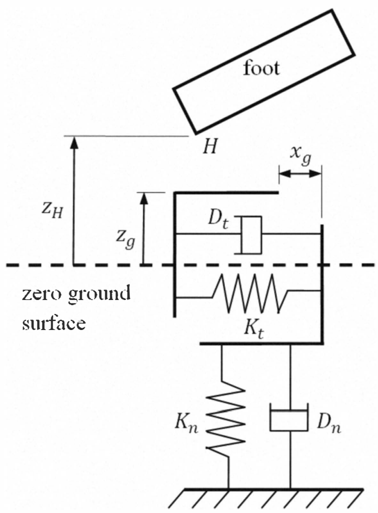

Fig. 2 Contact Model

1) Normal Forces

Contact normal forces can be computed by (1).

$$f_{czi} = \begin{cases} 0 & if\ z_{H_i} > z_g \\ max\ (0,\ -K_n z_g - D_n \dot{z}_{Hi}) & if\ z_{H_i} = z_g \end{cases} \quad (1)$$

Vertical motion of the ground surface z_g can be estimated by integration from the equation of motion of the ground along the vertical direction (2).

$$\dot{z}_g = -(K_n z_g + f_{czi})/D_n \quad (2)$$

2) Friction Forces

Friction forces can be computed by (3).

$$f_{cxi} = \begin{cases} -\mu f_{czi} & if\ f_{stick} < -\mu f_{czi} \\ \mu f_{czi} & if\ f_{stick} > \mu f_{czi} \\ f_{stick} & otherwise \end{cases} \quad (3)$$

Where f_{stick} is

$$f_{stick} = -K_t x_g - D_t \dot{x}_g \quad (4)$$

Eq. (5) is the equation of motion of the ground for tangential displacements. x_g can be obtained by integrating this equation.

$$\dot{x}_g = -(K_t x_g + f_{cxi})/D_t \quad (5)$$

C. Equations of Motion

Closed-form dynamic equations have to be written for the simulation of the system. In this study, the Lagrange method is used in obtaining the equations of motion. Position vectors required for kinematics are shown on Fig. 3.

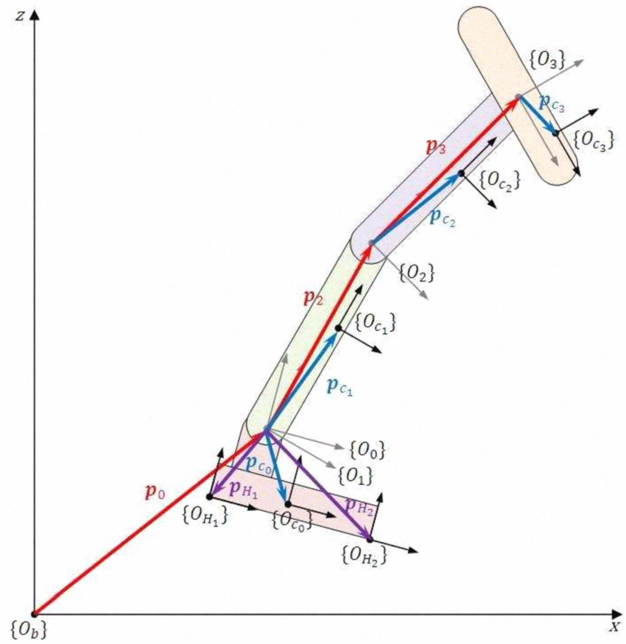

Fig. 3 Position Vectors Pointing the Origins of the Reference Frames

Expressions for position vectors pointing the origins of the reference frames $\{O_i\}$, $\{O_{c_i}\}$, $\{O_{H_i}\}$ are given below:

$${}^b\boldsymbol{p}_0 = \begin{bmatrix} x \\ 0 \\ z \end{bmatrix},\ {}^0\boldsymbol{p}_1 = \begin{bmatrix} 0 \\ 0 \\ 0 \end{bmatrix},\ {}^1\boldsymbol{p}_2 = \begin{bmatrix} 0 \\ 0 \\ l_1 \end{bmatrix},\ {}^2\boldsymbol{p}_3 = \begin{bmatrix} 0 \\ 0 \\ l_2 \end{bmatrix}$$

$$ {}^{0}\boldsymbol{p}_{C_0} = \begin{bmatrix} a_0 \\ 0 \\ c_0 \end{bmatrix},\ {}^{1}\boldsymbol{p}_{C_1} = \begin{bmatrix} a_1 \\ 0 \\ c_1 \end{bmatrix},\ {}^{2}\boldsymbol{p}_{C_2} = \begin{bmatrix} a_2 \\ 0 \\ c_2 \end{bmatrix},\ {}^{3}\boldsymbol{p}_{C_3} = \begin{bmatrix} a_3 \\ 0 \\ c_3 \end{bmatrix} $$

$$ {}^{0}\boldsymbol{p}_{H_1} = \begin{bmatrix} d_1 \\ 0 \\ s_1 \end{bmatrix},\ {}^{0}\boldsymbol{p}_{H_2} = \begin{bmatrix} d_2 \\ 0 \\ s_2 \end{bmatrix} \tag{6} $$

The mechanism is free to move on the x-z plane, therefore all rotations are about the y-axis. The unit vectors of the joints of the robot are given by:

$$ {}^{1}\boldsymbol{e}_1 = {}^{0}\boldsymbol{e}_1 = \begin{bmatrix} 0 \\ 1 \\ 0 \end{bmatrix},\ {}^{2}\boldsymbol{e}_2 = {}^{1}\boldsymbol{e}_2 = \begin{bmatrix} 0 \\ 1 \\ 0 \end{bmatrix},\ {}^{3}\boldsymbol{e}_3 = {}^{2}\boldsymbol{e}_3 = \begin{bmatrix} 0 \\ 1 \\ 0 \end{bmatrix} \tag{7} $$

Rotation matrices between successive frames are given by:

$$ {}^{b}_{0}\boldsymbol{R} = \boldsymbol{R}_y(\beta) \quad , \quad {}^{0}_{1}\boldsymbol{R} = \boldsymbol{R}_y(\theta_1) $$

$$ {}^{1}_{2}\boldsymbol{R} = \boldsymbol{R}_y(\theta_2) \quad , \quad {}^{2}_{3}\boldsymbol{R} = \boldsymbol{R}_y(\theta_3) \tag{8} $$

where $\boldsymbol{R}_y$ is

$$ \boldsymbol{R}_y(\alpha) = \begin{bmatrix} Cos\alpha & 0 & Sin\alpha \\ 0 & 1 & 0 \\ -Sin\alpha & 0 & Cos\alpha \end{bmatrix} \tag{9} $$

Angular velocities of the links are computed successively as follows:

$$ {}^{0}\boldsymbol{\omega}_0 = \begin{bmatrix} 0 \\ \dot{\beta} \\ 0 \end{bmatrix} $$

$$ {}^{1}\boldsymbol{\omega}_1 = {}^{1}_{0}\boldsymbol{R}\ {}^{0}\boldsymbol{\omega}_0 + \dot{\theta}_1\ {}^{1}\boldsymbol{e}_1 = \begin{bmatrix} 0 \\ \dot{\beta} + \dot{\theta}_1 \\ 0 \end{bmatrix} $$

$$ {}^{2}\boldsymbol{\omega}_2 = {}^{2}_{1}\boldsymbol{R}\ {}^{1}\boldsymbol{\omega}_1 + \dot{\theta}_2\ {}^{2}\boldsymbol{e}_2 = \begin{bmatrix} 0 \\ \dot{\beta} + \dot{\theta}_1 + \dot{\theta}_2 \\ 0 \end{bmatrix} $$

$$ {}^{3}\boldsymbol{\omega}_3 = {}^{3}_{2}\boldsymbol{R}\ {}^{2}\boldsymbol{\omega}_2 + \dot{\theta}_3\ {}^{3}\boldsymbol{e}_3 = \begin{bmatrix} 0 \\ \dot{\beta} + \dot{\theta}_1 + \dot{\theta}_2 + \dot{\theta}_3 \\ 0 \end{bmatrix} \tag{10} $$

Linear velocity of the origin of the reference frame $\{O_0\}$ is as follows:

$$ {}^{b}\boldsymbol{v}_0 = \begin{bmatrix} \dot{x} \\ 0 \\ \dot{z} \end{bmatrix} $$

$$ {}^{0}\boldsymbol{v}_0 = {}^{0}_{b}\boldsymbol{R}\ {}^{b}\boldsymbol{v}_0 = \begin{bmatrix} \dot{x}Cos\beta - \dot{z}Sin\beta \\ 0 \\ \dot{x}Sin\beta - \dot{z}Cos\beta \end{bmatrix} \tag{11} $$

Linear velocities of the origins of the reference frames $\{O_i\}$ and $\{O_{C_i}\}$ are can be computed successively by (12) and (13).

$$ {}^{1}\boldsymbol{v}_1 = {}^{1}_{0}\boldsymbol{R}\left({}^{0}\boldsymbol{v}_0 + {}^{0}\boldsymbol{\omega}_0 \times {}^{0}\boldsymbol{p}_1 \right) $$

$$ {}^{2}\boldsymbol{v}_2 = {}^{2}_{1}\boldsymbol{R}\left({}^{1}\boldsymbol{v}_1 + {}^{1}\boldsymbol{\omega}_1 \times {}^{1}\boldsymbol{p}_2 \right) $$

$$ {}^{3}\boldsymbol{v}_3 = {}^{3}_{2}\boldsymbol{R}\left({}^{2}\boldsymbol{v}_2 + {}^{2}\boldsymbol{\omega}_2 \times {}^{2}\boldsymbol{p}_3 \right) \tag{12} $$

$$ {}^{0}\boldsymbol{v}_{C_0} = {}^{0}\boldsymbol{v}_0 + {}^{0}\boldsymbol{\omega}_0 \times {}^{0}\boldsymbol{p}_{C_0} $$

$$ {}^{1}\boldsymbol{v}_{C_1} = {}^{1}\boldsymbol{v}_1 + {}^{1}\boldsymbol{\omega}_1 \times {}^{1}\boldsymbol{p}_{C_1} $$

$$ {}^{2}\boldsymbol{v}_{C_2} = {}^{2}\boldsymbol{v}_2 + {}^{2}\boldsymbol{\omega}_2 \times {}^{2}\boldsymbol{p}_{C_2} $$

$$ {}^{3}\boldsymbol{v}_{C_3} = {}^{3}\boldsymbol{v}_3 + {}^{3}\boldsymbol{\omega}_3 \times {}^{3}\boldsymbol{p}_{C_3} \tag{13} $$

Kinetic and potential energies of the system and the Lagrangian are computed as follows:

$$ T = \frac{1}{2}\sum_{i=0}^{3} m_i\ {}^{i}\boldsymbol{v}_{C_i}^{T}\ {}^{i}\boldsymbol{v}_{C_i} + \frac{1}{2}\sum_{i=0}^{3}\ {}^{i}\boldsymbol{\omega}_i^{T}\ {}^{C_i}\boldsymbol{I}_i\ {}^{i}\boldsymbol{\omega}_i \tag{14} $$

$$ V = -m_0\ {}^{b}\boldsymbol{g}^{T}\left[{}^{b}\boldsymbol{p}_0 + {}^{b}\boldsymbol{p}_{C_0} \right] - m_1\ {}^{b}\boldsymbol{g}^{T}\left[{}^{b}\boldsymbol{p}_0 + {}^{b}\boldsymbol{p}_1 + {}^{b}\boldsymbol{p}_{C_1} \right] - m_2\ {}^{b}\boldsymbol{g}^{T}\left[{}^{b}\boldsymbol{p}_0 + {}^{b}\boldsymbol{p}_1 + {}^{b}\boldsymbol{p}_2 + {}^{b}\boldsymbol{p}_{C_2} \right] - m_3\ {}^{b}\boldsymbol{g}^{T}\left[{}^{b}\boldsymbol{p}_0 + {}^{b}\boldsymbol{p}_1 + {}^{b}\boldsymbol{p}_2 + {}^{b}\boldsymbol{p}_3 + {}^{b}\boldsymbol{p}_{C_3} \right] \tag{15} $$

$$ \mathcal{L} = T - V \tag{16} $$

where $\boldsymbol{g}$ is the acceleration of gravity vector.

$$ {}^{b}\boldsymbol{g} = \begin{bmatrix} 0 \\ 0 \\ -g \end{bmatrix} \tag{17} $$

Generalized forces are obtained by applying virtual work principle as (18).

$$ Q_x = f_{cx1} + f_{cx2} $$

$$ Q_z = f_{cz1} + f_{cz2} $$

$$ Q_\beta = $$

$$ f_{cx1}(-d_1Sin\beta + s_1Cos\beta) + f_{cz1}(-d_1Cos\beta - s_1Sin\beta) + f_{cx2}(-d_2Sin\beta + s_2Cos\beta) + f_{cz2}(-d_2Cos\beta - s_2Sin\beta) $$

$$ Q_{\theta_1} = \tau_1 $$

$$ Q_{\theta_2} = \tau_2 $$

$$ Q_{\theta_3} = \tau_3 \tag{18} $$

Closed-form equations of motions can be written in matrix form.

$$ \boldsymbol{M}\ddot{\boldsymbol{\Theta}} + \boldsymbol{C} + \boldsymbol{G} = \boldsymbol{Q} \tag{19} $$

Where $\boldsymbol{M}$ is the inertia matrix, $\boldsymbol{\Theta}$ is the generalized coordinate vector, $\boldsymbol{C}$ is the vector of coriolis and centrifugal forces, $\boldsymbol{G}$ is the vector of gravitational forces, and $\boldsymbol{Q}$ is the vector of generalized forces. The forward dynamics of the system can be represented as follows:

$$ \ddot{\boldsymbol{\Theta}} = \boldsymbol{M}^{-1}[\boldsymbol{Q} - \boldsymbol{C} - \boldsymbol{G}] \tag{20} $$

III. Control

Jumping motion consist of flight and stance phases. Since the characteristics of dynamics governing these two phases are fundamentally different, different control methods must be used for each phase. Moreover, the modeling equations are highly nonlinear and it is almost necessary to make some simplifying assumptions in order to design a viable controller.

The already mentioned three term controller proposed by Raibert [5] is well adapted for the control of the one legged mechanism considered in this work. The controller consists of three parts: 1. Jumping height control, 2. Forward velocity control, 3. Body orientation control.

A. Flight Phase Controller

During the flight phase, the robot is a free flying serial mechanism and the only active forces acting on the system are joint torque and gravitational forces. Angular and linear momentum of the system are conserved in this phase. The flight phase can be considered as a preparation for the next contact phase. The flight phase controller must accomplish two tasks. The first task is the control of foot orientation which must be parallel to the ground at the start of the stance phase. The overall motion velocity depends on the landing position of the foot along the forward direction. The second task is the control of the foot position with respect to the concentrated mass. Therefore, the flight phase control can be considered as a trajectory generation and servo positioning problem. The following PD type joint controllers are used in flight phase.

$$\tau_i = K_p(\theta_{di} - \theta_i) + K_d(\dot{\theta}_{di} - \dot{\theta}_i) \qquad (21)$$

B. Stance Phase Controller

During the stance phase, ground forces have a dominant effect on the system dynamics. In this phase, the mechanism can be considered as a fixed base serial chain. This is the phase where the body orientation can be adjusted. The stance phase controller has to adjust the body orientation while maintaining the dynamic balance.

1) Dynamic Balance

Dynamic balance is a key issue in legged locomotion [14]. It prevents legged robots from falling down and turning over. A legged mechanism can be said to be in dynamic balance if the Zero Moment Point (ZMP) remains inside the support polygon during the stance phase. In this study, it is assumed that the system mass can be considered as a point mass concentrated at the hip joint. This is a commonly used approximation in order to simplify the governing equations [15, 7]. The ZMP position can be calculated by using the gravitational and inertial forces acting on the system. The ZMP is the point on the ground where total moment of all gravitational and inertial forces is zero. For our robot model, total mass of the robot is assumed to be accumulated at the hip joint. The assumption of concentrated mass at the hip level necessitates a mechanical structure with relatively light legs. All gravitational and inertial forces acting on the point mass model is shown on Fig. 4.

For this system position of the ZMP can be calculated as follows:

$$p_{ZMP} = x_c - \frac{\ddot{x}_c z_c}{\ddot{z}_c + g} \qquad (22)$$

Equation (22) is the equation establishes a differential relationship between the ZMP and CoM (Center of Mass) positions. This equation is non-linear and non-causal when the p_{ZMP} is output and x_c and z_c are the inputs of the system. Kajita derived Linear Inverted Pendulum Model by assuming z_c as constant [14]. In his study, he applied preview control on linear equations to overcome the non-causality problem.

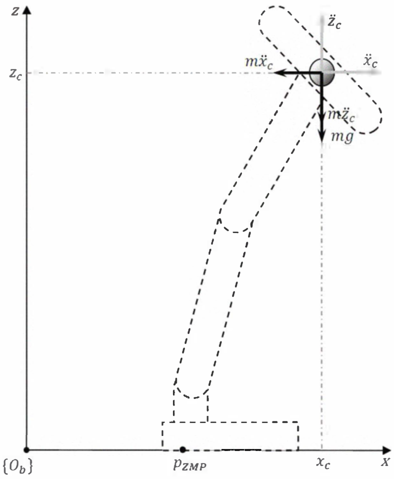

Fig. 4 Gravitational and inertial forces acting on the point mass

The ZMP equation shows also that the dynamics of the CoM motion is explicitly related to the ZMP position. Therefore control of ZMP position in stance phase can be interpreted as a kind of force control problem. The force applied to the CoM is directly related to the τ_1 and τ_2 joint torque through the Jacobian matrix with the following equation.

$$\begin{bmatrix}\tau_1\\ \tau_2\end{bmatrix} = \underbrace{\begin{bmatrix} l_1 Cos\theta_1 + l_2 Cos(\theta_1+\theta_2) & -[l_1 Sin\theta_1 + l_2 Sin(\theta_1+\theta_2)] \\ l_2 Cos(\theta_1+\theta_2) & -l_2 Sin(\theta_1+\theta_2)\end{bmatrix}}_{J^T} \begin{bmatrix} f_x \\ f_z \end{bmatrix} \qquad (23)$$

2) Control of the Body Orientation

The hip joint is used to adjust the body orientation during the stance phase. A simple PD controller is used for position control of this third joint. In order to hold the body upright position, the desired reference value is generated as follows:

$$\theta_{d3} = -\beta - \theta_1 - \theta_2 \qquad (24)$$

C. Force Control Approach and Virtual Spring Principle

In the previous section, the equation relating the first and second joint torque to the applied force to the point mass is derived. Now the problem is to determine an algorithm which generates the required forces for the dynamic balance. The virtual spring principle is exploited for this purpose [16]. The virtual spring is assumed to operate between the hip and ankle joints. Introduction of the virtual spring guaranties that the inertial force acting on the concentrated mass is partly directed to the ankle joint. Natural and actual lengths of the spring are denoted L_0 and L. The unit vector $\boldsymbol{e}_s$ along the spring shows the direction of the spring force. Magnitude of the spring force is determined by compression of the spring and spring constant K_s. Spring force vector is evaluated as follows:

$$ {}^b\boldsymbol{e}_s = ({}^b\boldsymbol{p}_2 + {}^b\boldsymbol{p}_3)/\mathrm{L} \tag{25}$$

$$ {}^b\boldsymbol{f}_s = K_s(L_0 - L)\, {}^b\boldsymbol{e}_s \tag{26}$$

Now it is possible to obtain the required joint torques generating virtual spring force.

$$\begin{bmatrix}\tau_1\\ \tau_2\end{bmatrix} = \boldsymbol{J}^T\, {}^b\boldsymbol{f}_s \tag{27}$$

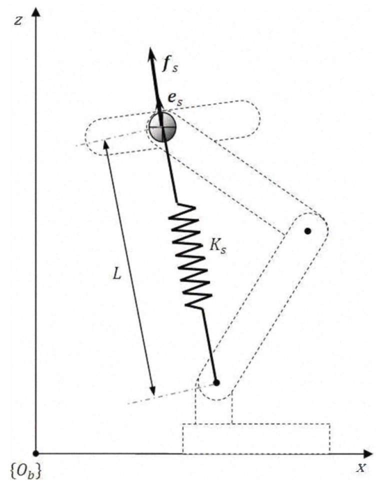

Fig. 5 Virtual Spring Force Vector

IV. Simulation Results

In this section, simulation results are presented for a model with following parameters:

$m_0 = 0.3kg, m_1 = 0.3kg, m_2 = 0.3kg, m_3 = 10kg$
$l_0 = 0.05m, l_1 = 0.3m, l_2 = 0.3m$
$a_0 = 0m, c_0 = l_0/2, a_1 = 0, c_1 = l_1/2$
$a_2 = 0, c_2 = l_2/2, a_3 = 0, c_3 = 0$
$d_1 = -0.1, s_1 = -l_0, d_2 = 0.1, s_2 = -l_0$
$K_{s_1} = 5000N/m, K_{s_2} = 8000N/m, L_0 = 0.5196m$
$K_p = 100, K_d = 4$
$K_n = 50000N/m, D_n = 180Ns/m$
$K_t = 100000N/m, D_t = 100Ns/m$

The ratio of body mass to leg mass is 11.11 which is 18 for Raibert's one-leg planar hopper [5].

The system's energy is being dissipated because of damping and friction at ground contact. To maintain motion, two different spring stiffness constant are used during the stance phase. The spring stiffness is shifted between K_{s1} and K_{s2} when the vertical velocity of the point mass is zero.

All initial velocities are zero and initial conditions for the generalized coordinates are as follows:

$x(0) = 0, z(0) = 0.5, \beta(0) = 0$
$\theta_1(0) = \pi/6, \theta_2(0) = -\pi/3, \theta_3(0) = \pi/6$

A desired forward velocity of $1m/s$ is used in simulations. Hip and ankle joint trajectories with CoM trajectory is shown on Fig. 6. As can be seen on the figure, CoM trajectory is very close to the hip trajectory.

Fig. 7 shows the joint torques. Maximum values occur in knee torque. This shows that the vertical acceleration of the body is mainly provided by the knee torque.

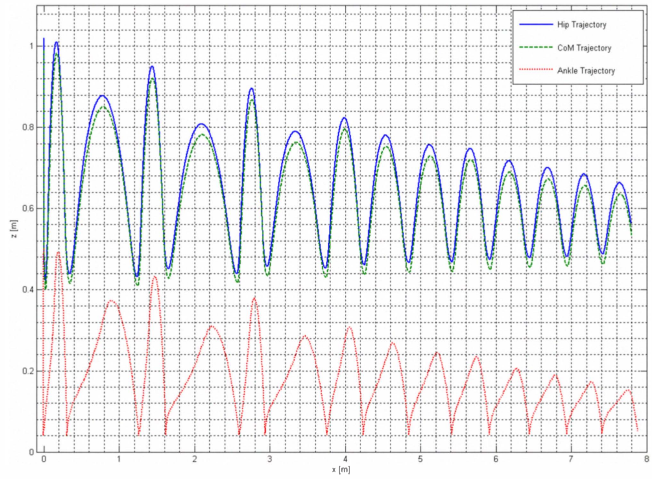

Fig. 6 Hip, ankle and CoM Trajectories on x-z plane [m]

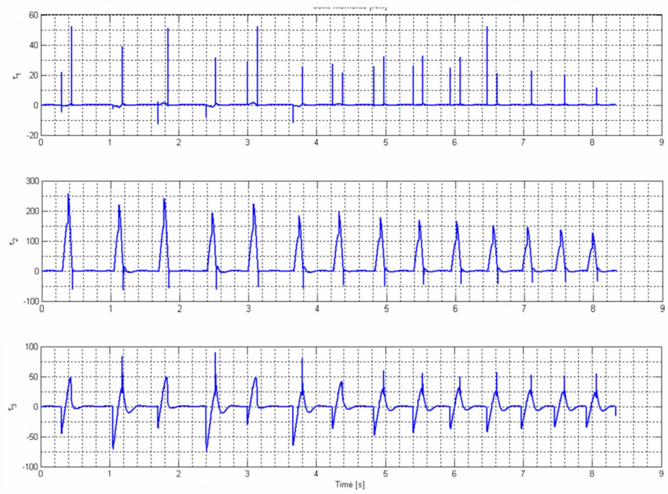

Fig. 7 Joint Moments (τ_1, τ_2, τ_3) [Nm] vs. Time [s]

The virtual spring force is presented on Fig. 8. The z component of the spring force dominates the x component.

Fig. 9 represents the friction forces f_{cx1} and f_{cx2} and normal forces f_{cz1} and f_{cz2}.

The ZMP trajectory is shown on Fig. 10. The gaps on the diagram show the flight phases. The ZMP travels from heel to toe during the stance phases.

The forward velocity of the hip joint is shown on Fig. 11. As can be seen from the diagram the desired velocity of 1m/s is accomplished after a transient of 5 hopping cycles.

V. Conclusion

One-legged jumping motion of 3 DoF leg mechanism has been modeled. Two controllers have been considered for flight and stance phases. Dynamical balance during the stance phase is controlled by the so-called virtual spring approach. Dynamic simulations show that the proposed control method results with satisfying jumping behavior where the mechanism achieves forward velocity 1m/s.

Results of this work constitute a basis for the design of a running biped prototype. The next step in the ongoing work is the design and construction of an experimental one-legged hopping mechanism.

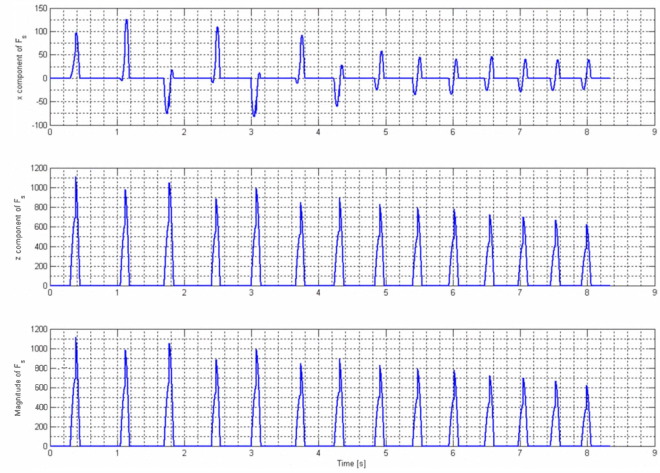

Fig. 8 x, z components, and magnitude of the Virtual Spring Force [N] vs. Time [s]

Fig. 9 Contact Forces (f_{cx1}, f_{cx2}, f_{cz1}, f_{cz2}) [N] vs. Time[s]

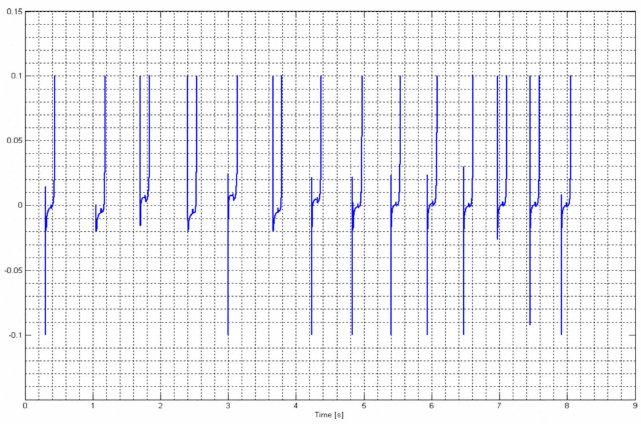

Fig. 10 ZMP Position Relative to the Foot Center [m] vs. Time [s]

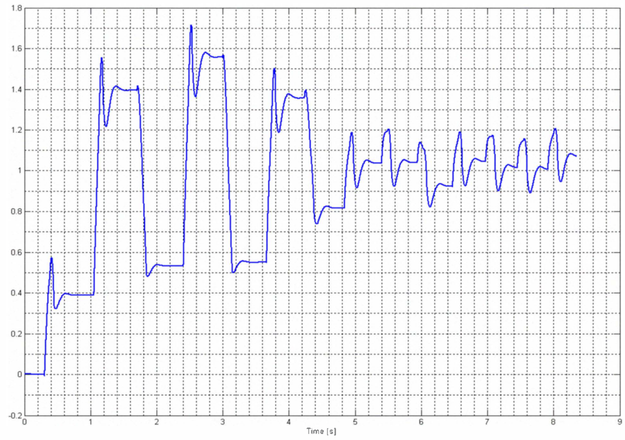

Fig. 11 Forward Velocity [m/s] vs. Time [s]

REFERENCES

[1] M. Hirose, K. Ogawa, "Honda humanoid robots development", *Philosophical Transactions of the Royal Society A*, vol. 365, pp. 11–19, Jan. 2007.

[2] H. Hirukawa Kanehiro, K. Kaneko, S. Kajita, K. Fujiwara, Y. Kawai, F. Tomita, S. Hirai, K. Tanie, T. Isozumi, K. Akachi, T. Kawasaki, S. Ota, K. Yokoyama, H. Handa, Y. Fukase, J. Maeda, Y. Nakamura, S. Tachi, and H. Inoue, "Humanoid robotics platforms developed in HRP", *Robotics and Autonomous Systems*, vol. 48, no. 4, pp. 165–175, 2004.

[3] F. Pfeiffer, "The TUM walking machines", *Philosophical Transactions of the Royal Society A*, vol. 365, pp. 109–131, 2007.

[4] M. Raibert, K. Blankespoor, G. Nelson, R. Playter and the BigDog Team, "BigDog, the Rough-Terrain Quadruped Robot", *Proceedings of the 17th World Congress, The International Federation of Automatic Control, 2008*.

[5] M. H. Raibert, *Legged robot that balance*, Cambridge, MIT Press, 1986.

[6] S. Kajita, T. Nagasaki, K. Kaneko, K. Yokoi, K. Tanie, "A hop towards running humanoid biped", in *Proceedings. ICRA'04*, 2004, paper 11.3.4, p. 109.

[7] A. Kawamura, C. Zhu, "One-leg jumping with virtual spring principle", in *Proceedings of the 2008 IEEE International Conference on. Humanoid Robots*, 2008, pp. 34-39.

[8] B. Uğurlu, A. Kawamura, "Online Running Trajectory Planning for Bipedal Robots based on ZMP and Euler's Equations", *Journal of System Design and Dynamics*, vol. 4, pp. 26-37, 2010.

[9] K. Nagasaka, Y. Kuroki, S. Suzuki, Y. Itoh, J. Yamaguchi, "Integrated motion control for walking, jumping and running on a small bipedal entertainment robot", *Proceedings of the 2004 IEEE ICRA*, pp.3189-3194, 2004.

[10] A. Sayyad, B. Seth, P. Seshu, "Single-legged hopping robotics research", *Robotica*, vol. 25, pp. 587-613, 2007.

[11] R. Tajima, K. Suga, "Motion having a Flight Phase: Experiments Involving a One-legged Robot", in *Proc. IEEE-RSJ Int. Conf. On Intelligent Robotics and Systems,* 2006, pp. 1726–1731.

[12] R. Tajima, D. Honda, K. Suga, "Fast Running Experiments Involving a Humanoid Robot", in *RSJ2008*, 2008.

[13] R. Featherstone, *Rigid Body Dynamics Algorithms,* Springer-Verlag New York Inc., 2008.

[14] M. Vukobratovic, B. Borovac, "Zero-moment point-thirty five years of its life", *International Journal of Humanoid Robotics,* vol.1, pp.157-173, 2004.

[15] S. Kajita, F. Kanehiro, K. Kaneko, K. Fujiwara, K. Harada, K. Yokoi, H. Hirukawa, "Biped walking pattern generation by using preview control of zero-moment point", *Proceedings. ICRA'03*, pp. 1620-1626, 2003.

[16] J. Pratt, C. M. Chew, A. Torres, P. Dilworth, G. Pratt, "Virtual model control: An intuitive approach for bipedal locomotion", *The International Journal of Robotics Research*, vol. 20, pp. 129, 2001